



HAL
open science

3D reconstruction of compressible flow by synchronized multi camera BOS

François Nicolas, Francis Micheli, David Donjat, Aurélien Plyer, Frédéric Champagnat, Guy Le Besnerais

► **To cite this version:**

François Nicolas, Francis Micheli, David Donjat, Aurélien Plyer, Frédéric Champagnat, et al.. 3D reconstruction of compressible flow by synchronized multi camera BOS. 18th International Symposium on applications of laser techniques to fluid mechanics, Jul 2016, LISBONNE, Portugal. hal-01385597

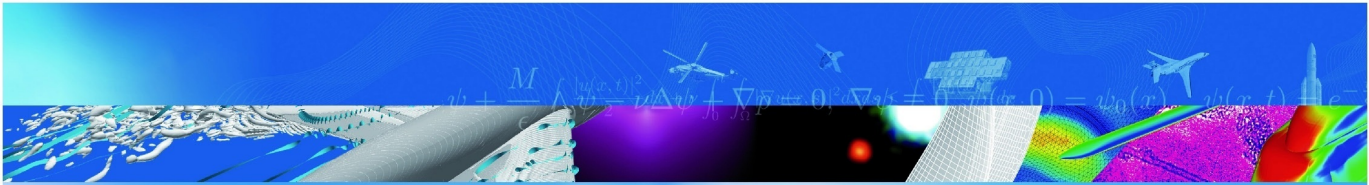
HAL Id: hal-01385597

<https://hal.science/hal-01385597>

Submitted on 24 Oct 2016

HAL is a multi-disciplinary open access archive for the deposit and dissemination of scientific research documents, whether they are published or not. The documents may come from teaching and research institutions in France or abroad, or from public or private research centers.

L'archive ouverte pluridisciplinaire **HAL**, est destinée au dépôt et à la diffusion de documents scientifiques de niveau recherche, publiés ou non, émanant des établissements d'enseignement et de recherche français ou étrangers, des laboratoires publics ou privés.



COMMUNICATION A CONGRES

**3D reconstruction of compressible
flow by synchronized multi camera
BOS**

F. Nicolas, F. Micheli, D. Donjat, A. Plyer,
F. Champagnat, G. Le Besnerais

18th International Symposium on applications of laser
techniques to fluid mechanics

LISBONNE, PORTUGAL

4-7 juillet 2016

TP 2016-628

70 2016
ans

ONERA

THE FRENCH AEROSPACE LAB

3D reconstruction of compressible flow by synchronized multi camera BOS

François Nicolas^{1,*}, Francis Micheli¹, David Donjat¹, Aurélien Plyer², Frédéric Champagnat², Guy Le Besnerais²

1: ONERA/DMAE, Toulouse, France

2: ONERA/DTIM, Palaiseau, France

* Correspondent author francois.nicolas@onera.fr

Keywords: BOS, Tomography, Underexpanded Jet

ABSTRACT

We have recently proposed an original one-step 3DBOS method for reconstruction of 3D density volume from a limited number of BOS images [7]. In this paper we investigate the application of this method to compressible flows. We first optimize the 2D BOS set up in order to mitigate the local harsh effect of blurring related to strong density gradients. We show that a careful choice of experimental conditions allows obtaining accurate deviation fields from 2D BOS images. We then apply our 3DBOS method on a bench involving 12 cameras and demonstrate physically consistent 3D reconstruction on mean field data for an underexpanded jet flow injected into a quiescent air. An instantaneous density field reconstruction has also been performed, demonstrating all the potential of the technique for physical analysis of the flow.

1. Introduction

Background Oriented Schlieren is a simple optical technique aiming at measuring density gradients. A textured background is recorded by a camera, firstly without flow. Then a second picture is taken with a phase object in between the camera and the background. The light rays deflections caused by refractive index variations leads to virtual displacements of the background pattern on the camera sensor. Those displacements can be computed using image correlation methods, such as PIV software, and the deviation maps can be derived from the geometry of the experiment.

From deviation maps recorded on the same flow from various viewpoints, the 3D density field can be reconstructed [2] [6] [8]. Recently, we have proposed a novel one-step approach for such 3D reconstruction [7]. In the line of [2], our technique is based on simultaneous acquisitions of the flow by several cameras. In [7] good results were obtained with 12 cameras on aerothermal test cases where weak density gradients conditions ensure the validity of the paraxial hypothesis for ray trajectories. Moreover, for such incompressible flows, the 3D temperature field can be

derived from the density providing a way to validate the reconstruction from independent temperature measurements [3].

While traditional schlieren has been extensively used for the study of transonic and supersonic flows, providing precise visualizations of shock waves, the extension of 3DBOS reconstruction is not straightforward and is limited by two difficulties. The first issue is related to the blurring effect associated with strong gradients in BOS images, which degrades the accuracy of estimated deviations. In [6] a solution based on correlation of color pattern is proposed. In the present work, we rely on classical graylevel images but we show that, with a careful choice of experimental conditions, deviation maps with high resolution, comparable to traditional schlieren visualization, can be obtained. The second issue is related to the paraxial approximation which is not valid anymore when shock waves are involved. Our goal is to measure the ability of the 3DBOS algorithm presented in [7] to deal with strong density gradients.

2. Investigation of compressible effects on a BOS experiment

Shock waves and more generally strong density gradients induce severe light ray deviations. As a consequence, astigmatism is generated causing some blurring on the image as it can be seen on Fig. 1.

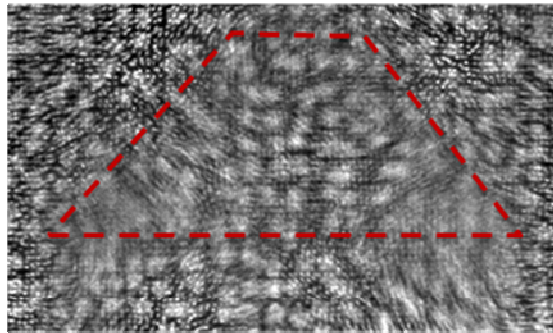


Fig. 1 Example of astigmatism effect induced by an underexpanded shock cell.

The blurring effect is damageable for image correlation methods: the correlation score decreases, and for severely blurred areas the estimation fails. Moreover, such missing deviations, even on restricted parts of the imaged field, can severely degrade the reconstruction of 3D density field. In this section, we study the effect of experimental choices both on the sensitivity and reliability of deviation estimation, and on local blur for the study of an underexpanded jet.

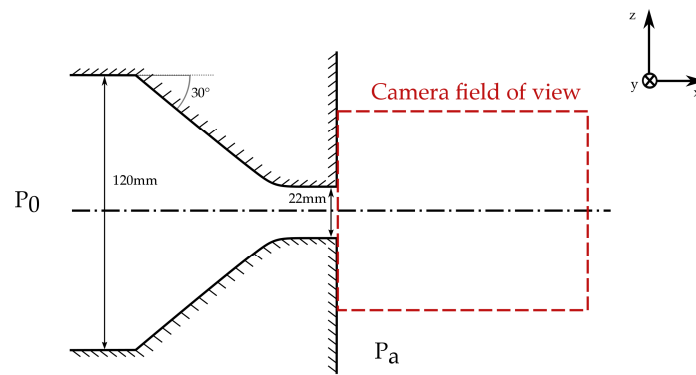


Fig. 2 Schematic view of the convergent nozzle generating our underexpanded jet.

Our facility consisted in a 22mm diameter convergent nozzle supplied by 9 bar pressurized air tank (see Fig. 2). Different Nozzle Pressure Ratios ($NPR = \text{jet total pressure} / \text{ambient static pressure}$) are investigated, ranging from 2 to 5. The air is regulated at a constant temperature equals to 20°C via a 570kW heater in order to prevent from condensation. The shape of the nozzle ensures a straight sonic condition on the jet exit. A JAI BM-500GE camera, equipped with a 70 mm lens, is placed at $Z_c = 1\text{m}$ from the nozzle whereas the background is moved between 18cm and 2.9m. For each position ($Z_b = 0.18\text{m}, 0.4\text{m}, 1.3\text{m}, 2.9\text{m}$), the background is designed in order to get 3-4 pixels dots on the camera image. The background is lighted with a Quantel Twins BSL double pulsed laser. Both pulses fire during the camera exposure time which leads to a better illumination. The effective exposure time is then equal to the delay between the two laser pulses (100ns).

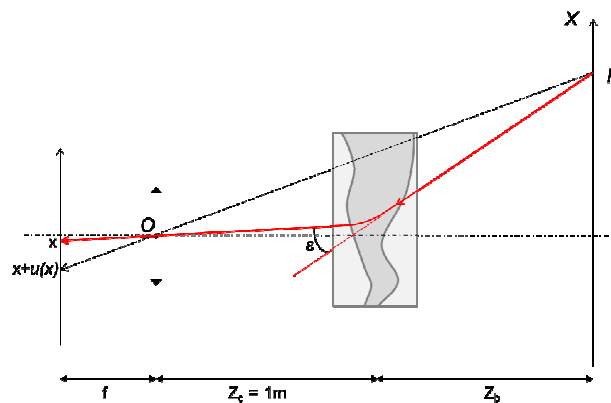


Fig. 3 BOS principle.

Two parameters have been studied: the influence of the background position and the effect of the camera aperture. As seen on the diagram presented in Fig. 3, the pixel displacement measured on the camera is proportional to the distance from the background to the flow.

Moving the background closer to the experiment reduces the effect of density gradients thus reduces the blurring effect.

Unfortunately, if a lower flow-background distance allows a better capture of shock waves, it also leads to a loss of sensitivity of the measurement process, at the risk of mitigation, or even complete elimination, of the small density gradients. We have tested various background positions and conducted an evaluation of the deviations estimation. From the four cases ($Z_b = 2.9, 1.4, 0.4$ and 0.18) we have selected the position $Z_b = 400\text{mm}$ as a good trade-off between the capture of small density variations such as acoustic waves and the ability of resolving high gradients associated to shock waves.

We will now focus on the aperture parameter influence. For each f-number (7.1, 8, 11, 16 and 22), the laser intensity has been adjusted to get the right amount of light. As the f-number increased, the astigmatism is reduced because the rays suffering from too large deviations do not enter the camera anymore. On Fig. 4, one can see the strong influence of the aperture: it not only allows a better correlation but reveals finer details on the flow topology which were hidden by the blurring effect. In this case, $f\# = 16$ represents the best choice. For larger f-numbers, diffraction impacts the resolution of the background, spreading the dots intensity and increasing correlation noise on BOS images.

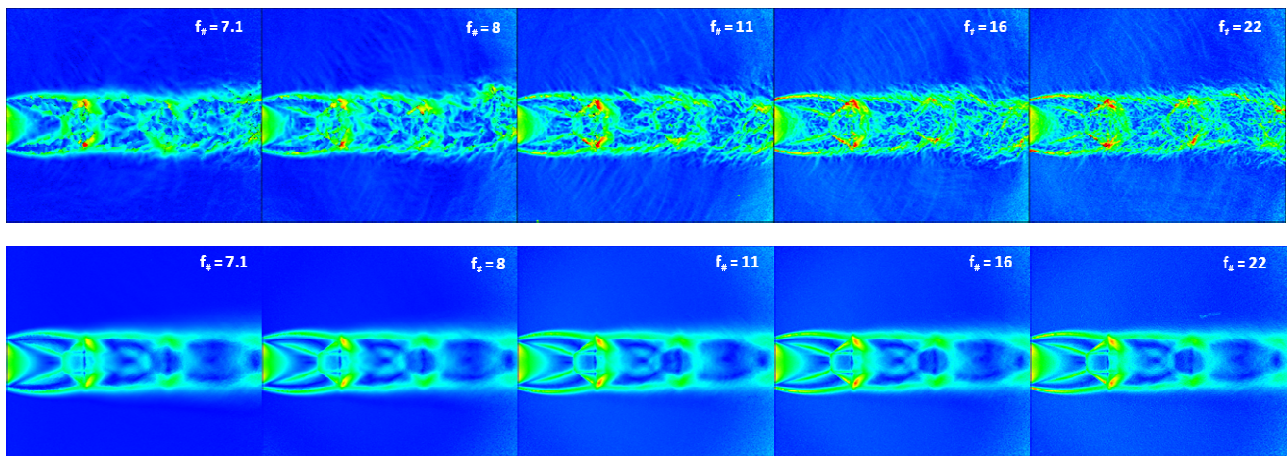


Fig. 4 Influence of the camera aperture on instantaneous BOS field (top) and mean field (bottom). Displacement norm in pixels (scale from 0 to 10).

In conclusion of this 2D study, by choosing wisely its set up, one can acquire very good quality BOS images, with a spatial resolution comparable to traditional schlieren visualization, as demonstrated on Fig. 5.

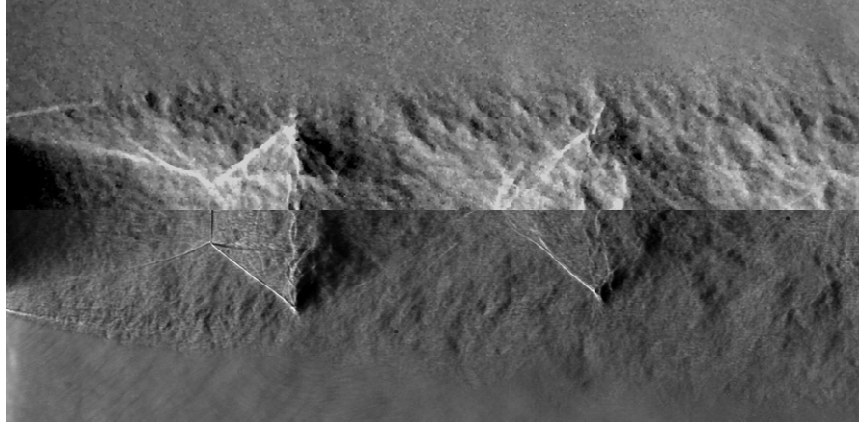


Fig. 5 Comparison between BOS image (top) and schlieren image (bottom). NPR=5.

3. Underexpanded jet 3D density field acquisition

We build our 3D BOS experiment based on the empirical study conducted for 2D BOS in the previous Section. Four background plates covered with 0.2mm dots are placed at a distance $Z_c=400\text{mm}$ of the jet. For the study of jets, placing the cameras on half a ring is the configuration chosen by most previous references ([7] [2]). We follow this line by setting up our 12 cameras on a hexagonal bench at a distance $Z_b=1000\text{mm}$ of the jet (see Fig. 6). The range of NPR condition is defined from 2 to 5.

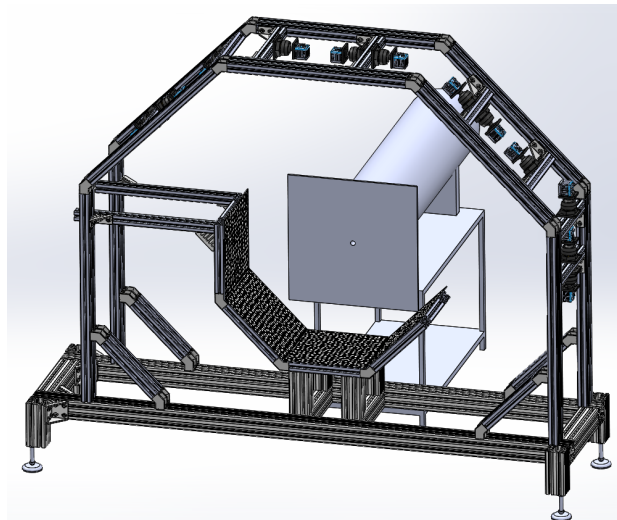


Fig. 6 3D BOS bench and supersonic hot jet facility.

A PIV laser is still used as light source, but now we split the beam into four before spreading each one on the backgrounds. This solution enables to cover the 4 background patterns as a

whole. As in the previous 2D case, the two laser pulses are used during the exposure time, both 12 cameras and laser are synchronized with a TTL pulse generators. Unfortunately, the amount of light remaining for each camera does not allow us to use the optimal f-number of 16 and we will operate the cameras at $f\#=8$. This choice leads to some filtering of fine scale structures, but as we are interested here in the reconstruction of mean density field, this loss is less critical as it can be seen on the mean field comparison on Fig. 4. Currently, ongoing work focuses on the set-up improvement in order to increase the amount of light recorded by the cameras and to work at higher f-numbers. This enhancement will be very relevant for the reconstruction of instantaneous flow field, especially at high NPR.

During the acquisition, images are transferred to the RAM memory via an Enterasys switch and then moved to SSD disks. This solution enables us to acquire images at 10Hz.

Finally, the multi cameras system is calibrated as explained in [9] by moving a 2D white calibration plate cover with black dots into the common volume of the cameras.

4. Results

In the current section we present both an average and instantaneous reconstruction for a moderately underexpanded jet (NPR=2) and the mean field of a strongly underexpanded jet (NPR=5). The NPR=5 mean field contains very high gradients. It has a well-defined topology and is less complex than the instantaneous one. Moreover, it can be compared with numerous previous works and with CFD simulations. With the actual set up, strong astigmatism effects prevent us to reconstruct satisfactory results on the instantaneous case.

Average 3D reconstructions are performed from the mean displacement field of each camera resulting of the average of 900 samples. The calculation is done over a volume of $10\times 7\times 7$ cm³ using between 40 and 100 million of 0.2 mm side voxels. A 3D mask is also used to help the reconstruction. As explained in [7], the solution to this inverse problem is defined as the minimizer of a compound criterion made of a least square data term penalized with a L2 criterion on density gradients. The regularization parameter λ is chosen accordingly to the L-curve strategy [5]. Compared to aerothermal cases which were considered in [7], the selected parameter is much lower here, ($\lambda=10^{-6}$ compared to $\lambda=10^{-4}$ in [7]) preventing from smoothing strong density gradients.

On the mean field of the moderately underexpanded jet, the train of shock wave is clearly visible in the potential core region. This pattern results from the successive reflection of expansion fan and shock wave on the jet boundary. The result being limited to the intersection

volume of all cameras, the very beginning of the jet is not reconstructed. The 3D mask edges visible on Fig. 7 might denote a lack of iterations in the reconstruction process to allow the regularization to smooth those artifacts. If our code perform well in this case, it is important to observe the existence of artifacts in the first two shock plane.

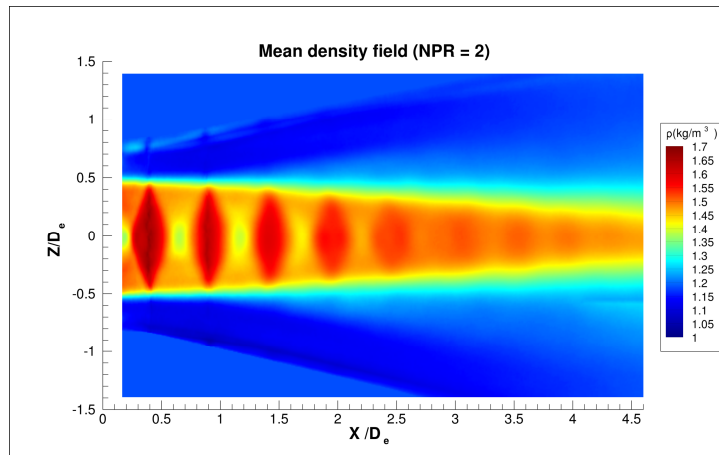


Fig. 7 Mean density field reconstruction for NPR=2 case. Slice at $y=0$.

The instantaneous reconstruction presented in Fig. 8, shows much more complexity. If the first two cells are quite stable (as we compare with the mean field) this is not the case for the following ones. One can also notice the instability of the second part of the jet where shock cells aspect is completely distorted. Some over-smoothing on the reconstruction also impacts the quality of the result and the capture of finer scales.

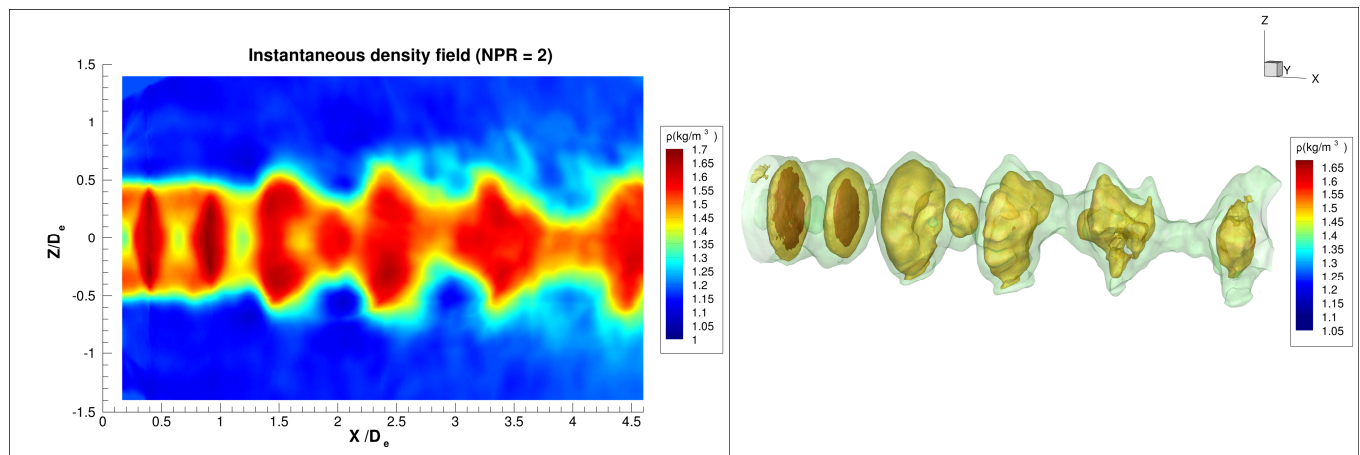


Fig. 8 Instantaneous density field reconstruction for NPR=2 case. Slice at $y=0$ on the left and iso-density on the right.

A good way to finer analyze our algorithm performance is to apply our direct operator on the reconstructed density field and compare the resulting deviation maps to the input ones. As it can be seen on Fig. 9, there is good agreement between synthesized deviations and measured ones.

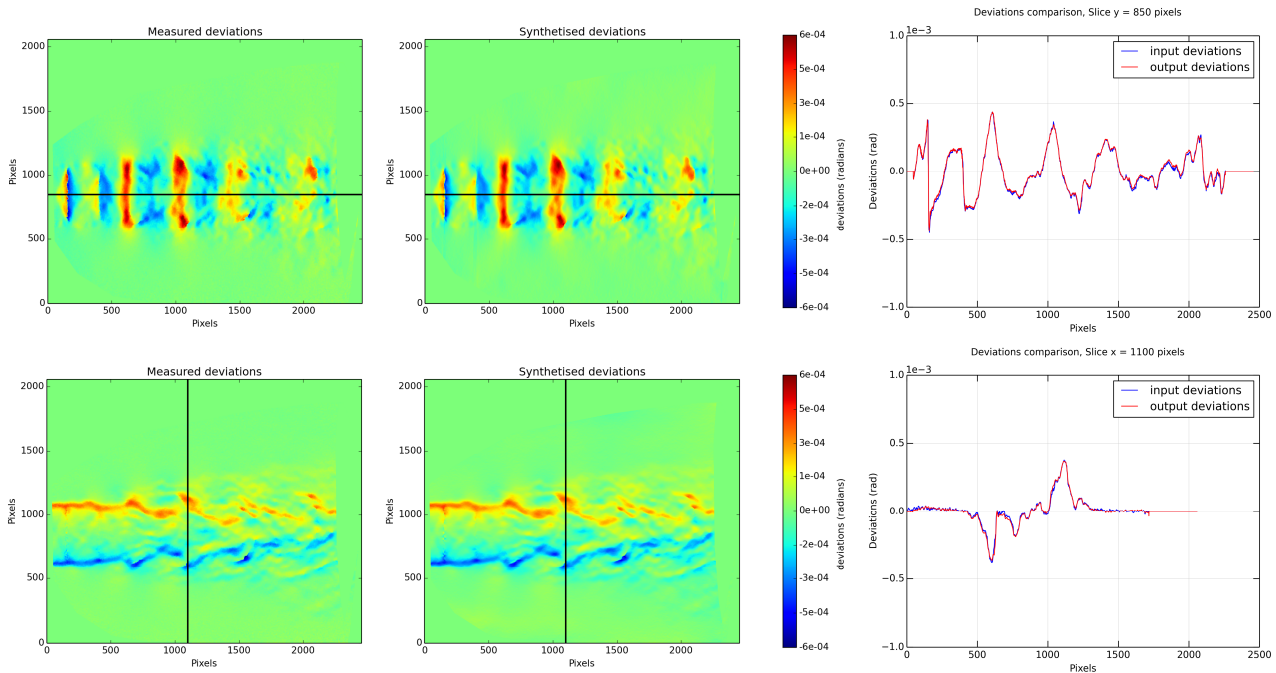


Fig. 9 Deviation map comparisons for ε_x map at the top and ε_z map at the bottom.

Because the use of a relatively large aperture doesn't seem to damage the average displacement fields, we push further our algorithm by reconstructing the mean field of a highly underexpanded jet with NPR=5. The reconstructed 3D density field is presented on the upper part of Fig. 10 and compared to a RANS simulation performed with FLUENT14 below. As we increased the NPR, a Mach disk (MD) appears. It can be seen on the two shock cells reconstructed. Behind the normal shock of the MD a subsonic zone is present. Then, the flow re-accelerated before encountering a new MD.

The 3D BOS reconstruction shows a very good agreement with the computation. Topology as well as the density levels is recovered. However, sharp density gradients are over-smoothed by the reconstruction process. Although the position of the MD seems different for the BOS reconstruction and the CFD on the left part of Fig. 10, the computation of density gradient on right part show a good agreement. Nevertheless, there is a difference between the computation and the 3D BOS result in the position of the second shock wave. This issue might be related the CFD result (as this configuration is still a challenging numerical problem) and the known difficulty to well recover the position of the second MD.

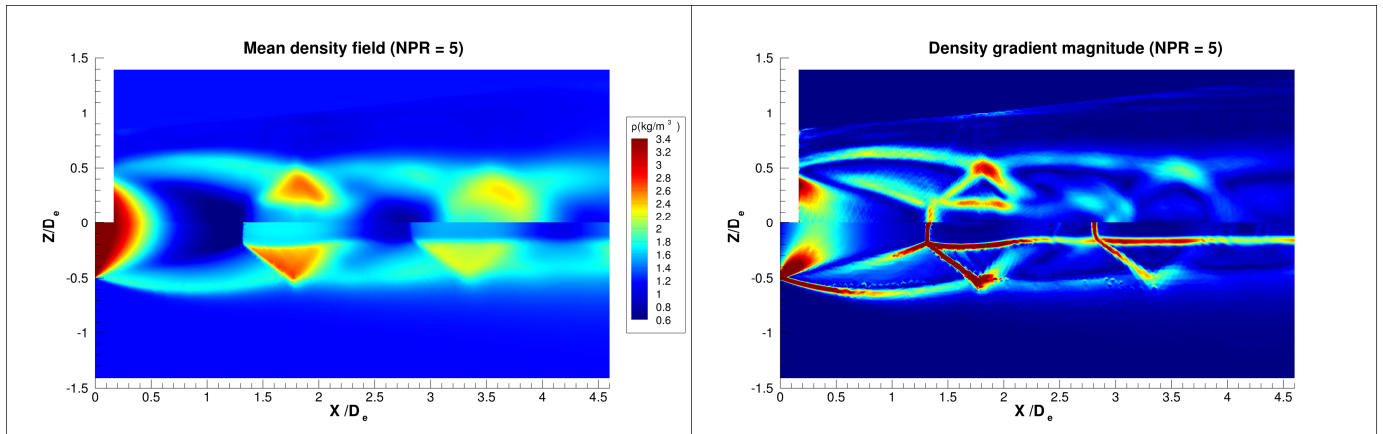


Fig. 10 Mean density field reconstruction for NPR=5 case on the left and Density gradient magnitude on the right. Slice at $y=0$. 3D BOS reconstruction on the upper part and RANS simulation on the lower part.

We also compared in Fig. 11 the position of the MD and his diameter with both schlieren measurements realized previously on the same underexpanded jet and [1]. Although the geometry of the Mach disk is over-smoothed by the reconstruction process, the location and size are quite consistent with this experimental database. Finally, we can also notice that the subsonic region behind the MD is well captured by our technique whereas the Abel inversion and schlieren CT of Takano [10] show some difficulties in this particular region. Moreover, our reconstruction highlights the ring shape of the reflected shock.

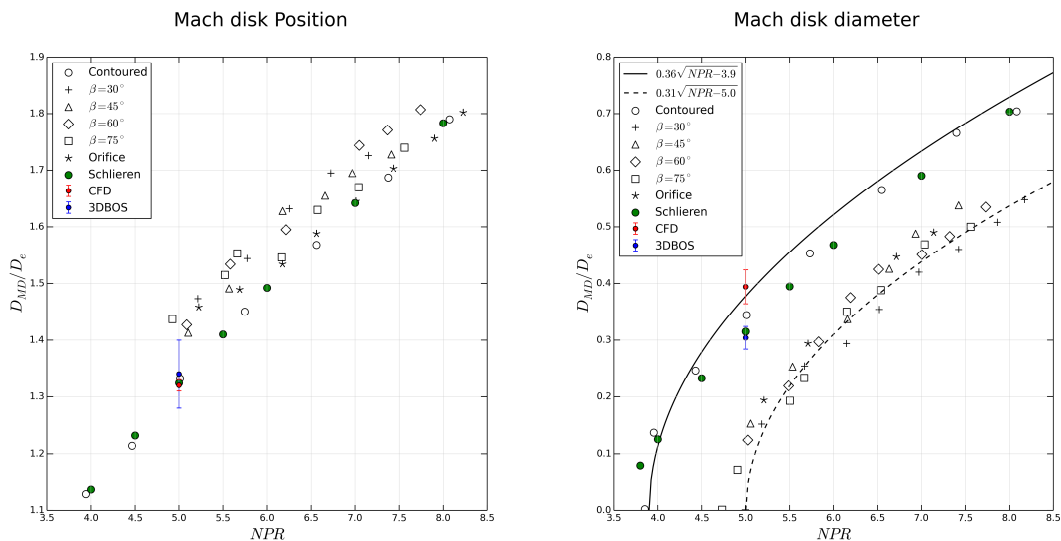


Fig. 11 Evolution of the Mach disk position and diameter with respect to the NPR from [8]. Comparison with the RANS simulation and our schlieren and 3D BOS measurement.

5. Conclusion

This paper focuses on 3D reconstructions of a compressible jet by BOS. Our contribution is two-fold. First, we have demonstrated that using an optimized set-up and assuming that illumination is sufficient to choose a large aperture number, good quality BOS image can be recorded, leading to estimated deviation of resolution close to schlieren techniques. Second, we have built a 3D BOS experiment involving 12 cameras mounted around an underexpanded jet so as to conduct a preliminary evaluation of the 3DBOS methods of [7] in compressible conditions. The results are very promising. The estimated flow is slightly oversmoothed, as the result of various choices, both in the deviation estimation step and in the reconstruction step. Getting more accurate estimation of deviation is mainly a matter of further improving the experimental set-up, but modification of the correlation method, and in particular use of pixelwise optical flow methods developed in Computer Vision could also bring further gains. However, on-going work focuses on the reconstruction part in order to circumvent the paraxial hypothesis and avoid oversmoothing of the density gradients by the regularization term.

To conclude, measurement of 3D density fields for compressible applications is very challenging. It is also a great interest for comparison with CFD computation and might be a way to better understand light distortion through shock waves. Particle position errors and velocity errors in supersonic PIV could benefit from such measurements and might be corrected with BOS [4].

5. Bibliography

- [1] Addy, A. L. (1981). Effects of axisymmetric sonic nozzle geometry on Mach disk characteristics. *AIAA Journal*, 19(1), 121-122.
- [2] B. Atcheson, W. Heidrich and I. and Ihrke, "An evaluation of optical flow algorithms for background oriented schlieren imaging.", *Experiments in fluids*, pp. vol. 46, no 3, p. 467-476., 2009.
- [3] D. Donjat, F. Nicolas, A. Plyer, F. Micheli, P. Cornic, G. Le Besnerais, F. Champagnat, Y. Le Sant, J.M. Deluc (2015) "Study of a co-flowing hot jet: an application of direct 3DBOS technique in research wind tunnel", 10th Pacific Symposium on Flow Visualization and Image Processing (PSFVIP 2015), Naples.
- [4] G. Elsinga, B. Van Oudheusden and F. Scarano, "Evaluation of aero-optical distortion effects in PIV.", *Experiments in fluids*, vol. 39, no. 2, pp. 246-256, 2005.

- [5] P. C. Hansen, «Analysis of discrete ill-posed problems by means of the L-curve.», SIAM review, vol. 34, n° 14, pp. 561-580, 1992.
- [6] F. Leopold, M. Ota, D. Klatt and e. al., "Reconstruction of the Unsteady Supersonic Flow around a Spike Using the Colored Background Oriented Schlieren Technique.", Journal of Flow Control, Measurement & Visualization, pp. 1(2), 69–76, 2013.
- [7] F. Nicolas, V. Todoroff, A. Plyer, G. Le Besnerais, D. Donjat, F. Micheli and F. Champagnat, "A direct approach for instantaneous 3D density field reconstruction from Background Oriented Schlieren (BOS) measurements.", Experiments in fluids, In press.
- [8] M. Ota, K. Hamada, H. Kato and e. al., "Computed-tomographic density measurement of supersonic flow field by colored-grid background oriented schlieren (CGBOS) technique.", Measurement Science and Technology, pp. vol. 22, no 10, p. 104011., 2011.
- [9] Y. Le Sant, V. Todoroff, A. Bernard-Brunel, G. Le Besnerais, F. Micheli and D. Donjat, "Multi-camera calibration for 3DBOS.", in 17th International Symposium on Applications of Laser Techniques to Fluid Mechanics, 2014.
- [10] Takano, H., Kamikihara, D., Ono, D., Nakao, S., Yamamoto, H., & Miyazato, Y. (2016). "Three-dimensional rainbow schlieren measurements in underexpanded sonic jets from axisymmetric convergent nozzles". Journal of Thermal Science, 25(1), 78-83.

